

# Electromagnetic Compatibility of a Low Voltage Power Supply for the ATLAS Tile Calorimeter Front-End Electronics

G. Blanchot<sup>a</sup>, U. Blumenschein<sup>d</sup>, I. Hruska<sup>a</sup>, I. Korolkov<sup>d</sup>, B. Palan<sup>a</sup>, J. Pontt<sup>c</sup>, A. Toro<sup>c</sup>, G. Usai<sup>b</sup>

<sup>a</sup>CERN, CH-1211 Geneva 23, Switzerland

<sup>b</sup>Enrico Fermi Institute, University of Chicago, USA

<sup>c</sup>UTFSM, Valparaiso, Chile

<sup>d</sup>IFAE, Universitat Autònoma de Barcelona, Spain

## Abstract

The front-end electronics of the ATLAS Tile Calorimeter is powered by DC/DC converters that sit close to it. The performance of the detector electronics is constrained by the conducted noise emissions of its power supply. A compatibility limit is defined for the system. The noise susceptibility of the front-end electronics is evaluated, and different solutions to reduce the front-end electronics noise are discussed and tested.

## I. POWER DISTRIBUTION SCHEME FOR THE TILE CALORIMETER

The front-end electronics of the Tile Calorimeter [1] is organized in drawers that are inserted in detector modules. Each drawer is 3 meter long and contains the front-end analogue and digitizing electronics for 45 photomultiplier tubes [2] in the case of the barrel modules. It is powered by eight regulated low voltage lines, and it is rated to consume a maximum power of 300W.

Because a drawer requires a tight voltage regulation on its power lines, the low voltage power supply was designed to fit in its vicinity, as an extension of it. The environmental constraints such as radiation and magnetic field tolerance were solved with the design of custom DC/DC converters that are remotely controlled by an ELMB [3]. The power supply is located in a closed volume known as *finger*. The power supply is water cooled.

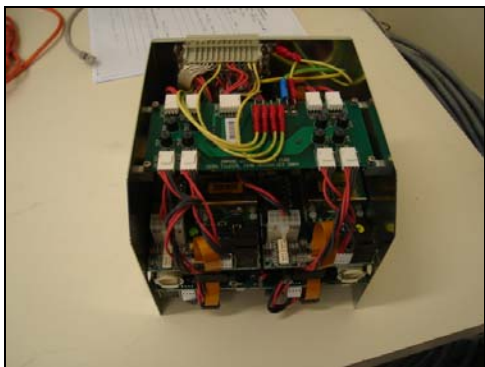


Figure 1: Finger low voltage power supply of the ATLAS Tile Calorimeter.

The finger low voltage power supplies (figure 1) are fed by bulk power supplies (200VDC) located in a control room. Auxiliary power supplies in the same control room are also required to power separately the monitoring and control circuitry. The power system (figure 2) is controlled by the Detector Control System (DCS) through a CANBus line that communicates with the ELMB of the power supply.

The low voltage outputs are isolated from earth, but all the return lines are put in common inside the drawer.

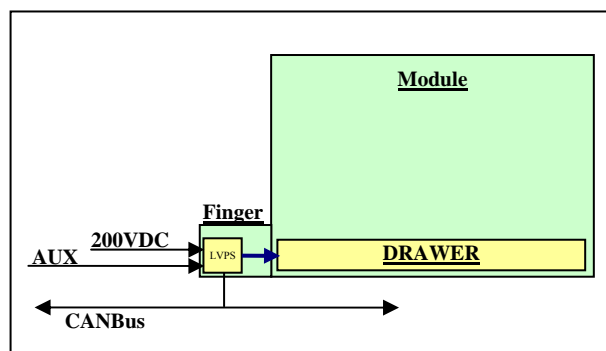


Figure 2: Tile Calorimeter power distribution scheme.

## NOISE PERFORMANCE TEST METHODS

The front-end noise is composed by the drawer electronics noise, by the power supply noise and by the external couplings on the interconnecting cables (not studied here).

### A. System Noise.

The achievable performance of the drawer electronics in terms of noise is limited by design. The system noise in each front-end channel was measured in detail on drawers that were powered with low noise linear power supplies. The system noise is evaluated in terms of high frequency and low frequency contributions from the data taken with the full data acquisition chain.

The high frequency noise seen by the fast readout electronics is estimated from the pedestals data. The estimation is based on a selection of parameters computed over several runs and on all the channels of a drawer:

- RMS of the pedestals distribution.
- Gaussian property of the pedestals distribution.

The low frequency noise is evaluated from data sampled by the current integrators ADC. Since the data is sampled sequentially channel by channel, correlation figures between channels are the best method to track low frequency noise.

The system noise requirements are specified as:

- High gain fast readout:  $RMS \leq 1.5$  counts.
- Slow integrators readout:  $RMS \leq 2.0$  counts (for any given gain).

### B. Noise Properties of the Converters.

A DC to DC converter is a source of high frequency noise in the form of common mode current sent to the load. The measurement of the output common mode current into a nominal resistive load allows evaluating the noise performance of a given power converter [4]. The measurement is made on the output of each converter or on the entire voltage bundle, with a calibrated current probe and an EMI receiver (figure 3). The obtained spectrum is then compared with respect to the limit lines specified in the ATLAS EMC policy [4].

The measurement of the total common mode current that enters the drawer electronics and that returns through the steel is measured with the same setup on the low voltage bundle that feeds the drawer.

The low frequency noise is contributed by the output ripple and it varies with the applied load. It is easily measured with an oscilloscope under nominal load conditions.

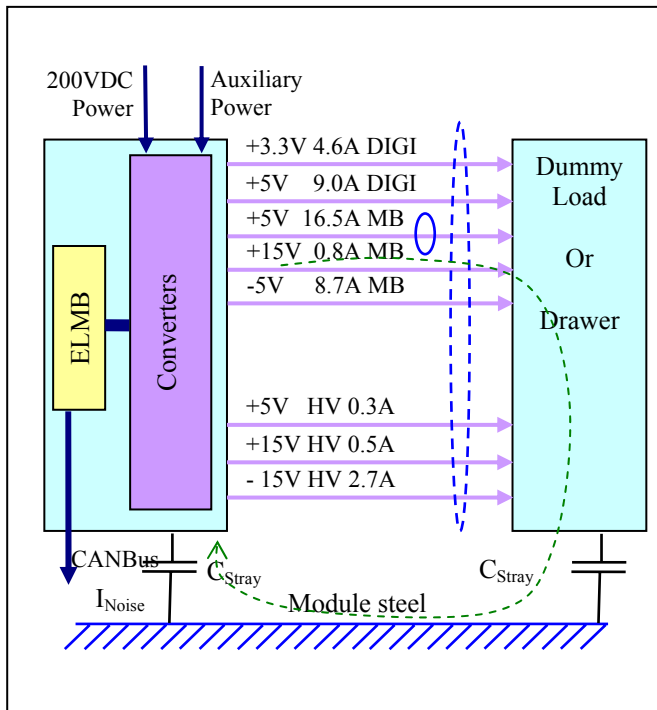


Figure 3: Finger power supply outputs ratings and common mode current measurement method on individual output (plain) or on the whole bundle (dashed). Stray capacitances couple noise currents to the module.

## NOISE MEASUREMENTS

The noise performance of the finger low voltage power supply (FLVPS) is compared with the equivalent performance of a temporary commercial, off-the-shelf, switched mode power supply used for the commissioning of the drawers in the ATLAS cavern. The system noise achieved with the temporary power supply and a linear power supply are equivalent. The measurements techniques, tools and reference limits considered here are defined in the ATLAS EMC Policy [3].

### A. High frequency noise susceptibility.

The measurement on individual outputs connected to a reference load showed that (figure 4):

- Both power supplies exhibit large common mode currents at the main switching frequency and associated harmonics, exceeding by 40 dB the limits in use.
- Above 1 MHz, the FLVPS emits 20dB more common mode current than the temporary LVPS.

The measurement on the whole low voltage bundle showed that (figure 5):

- The switching noise current stays below the limit and is smaller than the same current as measured on individual outputs.
- Above 1 MHz, the FLVPS exhibits up to 40 dB more noise current than the temporary power supply.

The switching noise current of a given converter returns through the cables of the others because they share a common return at the level of the load. The switching noise current path is comprised between the power supply and the common ground point, with a limited impact on the front-end performance.

At higher frequencies, the noise current propagates towards the front-end electronics of the drawer, and reaches the steel of the module through stray capacitances. The module provides a very low inductive return path to the power supply. Because of this, the noise current of each one of the converters is summed up. The high frequency noise current degrades the performance of the front-end electronic.

The larger system noise is expected close to the point where the converters return lines are put in common, namely in the vicinity of the patch panel (figure 6). The noise current leaves the drawer through stray capacitances to the steel, and its magnitude decreases as the distance from the common grounding point increases. This is clearly observed from the raw data (figure 6).

The excess of common mode current also results in a non Gaussian pedestals distribution (figure 7). The non Gaussian part of it is highly correlated for different channels, resulting in an undesirable impact on the jet energy measurements.

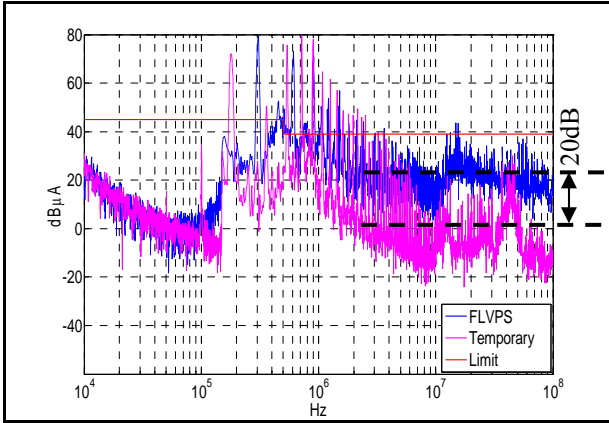


Figure 4: typical single output common mode current.

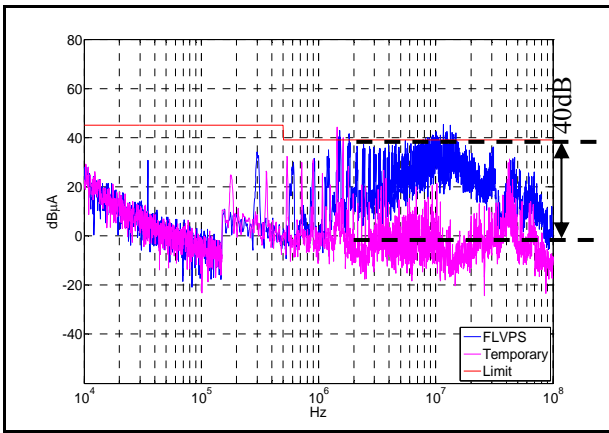


Figure 5: typical LV bundle common mode current.

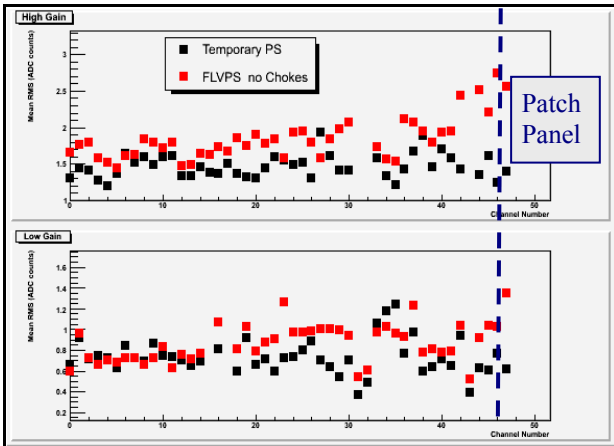


Figure 6: Pedestals RMS distribution across a drawer (patch panel on the right hand side).

### B. Filtering of high frequency noise.

To reduce significantly the amount of common mode current sent to the drawer, the common mode impedance of the converter output must be increased in the frequency range where the front-end electronics is most susceptible to noise.

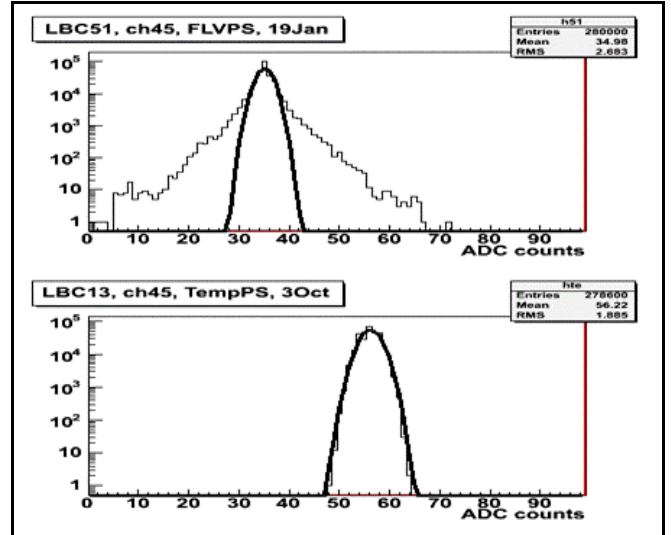


Figure 7: non Gaussian distribution of pedestals when using the unfiltered finger power supply (top) versus Gaussian distribution when using a commercial power supply (bottom).

First, common mode chokes placed on each converter output turned out to be the most efficient way to reduce the common mode current. The selected chokes, rated to 10A, offered an attenuation of more than 20 dB from 100 kHz to 10 MHz (figure 8). The common mode current on the output of each converter was brought below the limit in the switching frequency range and above 10 MHz, and the resulting noise distribution got better than with the temporary power supply (figures 9 and 10). However, because the chokes must be sized for the full load current, they require a non negligible volume that is unavailable for the finger power supply.

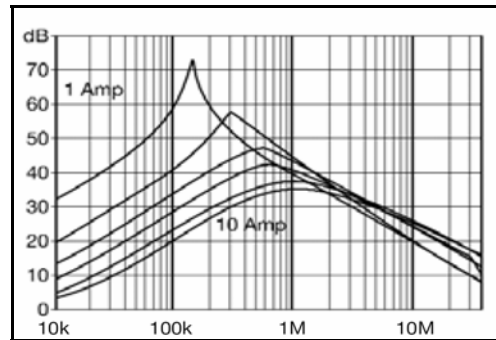


Figure 8: attenuation chart for typical common mode chokes.

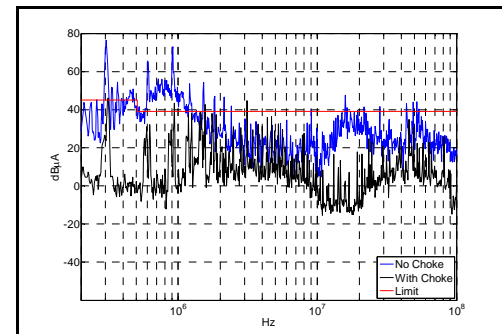


Figure 9: with a 10A common mode choke the single output common mode current is 20 dB below the ATLAS limit.

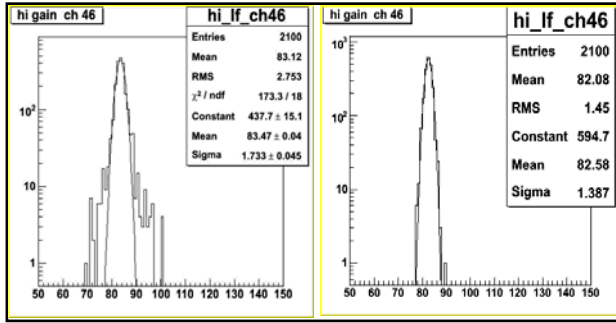


Figure 10: a common mode choke allows recovering the Gaussian property of the high gain fast readout pedestals distribution and its RMS to less than 1.5 counts.

As an alternative, a combination of carefully selected ferrites placed on each low voltage pair allowed to block significantly the common mode current too. The impedance curve of the selected ferrite exceeds  $50 \Omega$  between 3 MHz and 500 MHz (figure 11). The addition of two ferrites on the output of each converter allows the attenuation of its common mode current by up to 20dB between 1 MHz and 100 MHz (figure 12). The RMS of the pedestals distribution is improved and the Gaussian property is recovered (figure 13).

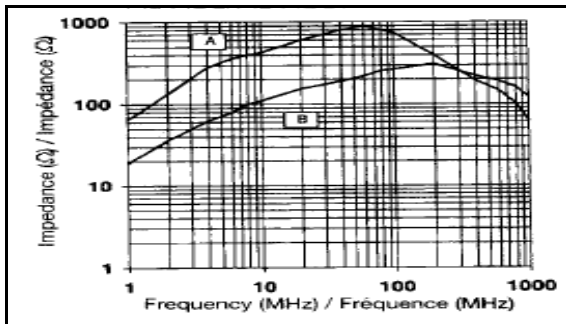


Figure 11: typical ferrite impedance curve for one turn (B) and two turns (A).

It must be noted that the ferrites are only effective above a few MHz, while the chokes offered an extended attenuation down to 100 kHz. However the results are very similar: therefore the drawer electronics is susceptible to high frequency noise above 1MHz, and the switching noise only plays a secondary role in the noise performance.

The power supply must operate in the presence of a magnetic field. No degradation of the ferrite properties was observed when exposing the ferrites to a nominal magnetic field of 200 Gauss.

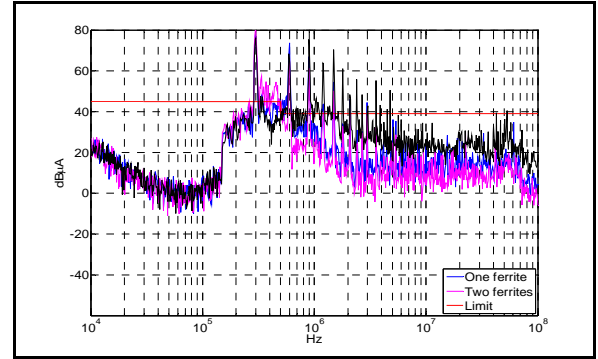


Figure 12: single output attenuation using one (blue) and two ferrites (pink).

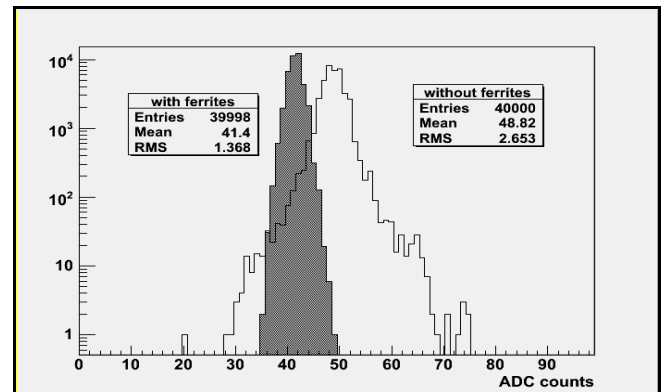


Figure 13: recovery of Gaussian distribution of pedestals using two ferrites on all low voltage outputs.

### C. Low frequency noise susceptibility.

The slow integrator system of the drawer electronics is designed to scan the average current of the 45 front-end photomultiplier tubes at a rate of 100 Hz. This system turned out to be sensitive to low frequency noise (below 10 kHz) on the low voltage power lines. In this frequency range the differential mode noise dominates in the form of voltage ripple. The correlation factor (Equ. 1) between the distributions of integrators pedestals for two different channels put in evidence the presence of a periodic, low frequency ripple that is added to the sampled voltages.

$$\rho_{i,j} = \frac{\text{cov}(i,j)}{\sigma_i \cdot \sigma_j} \quad [\text{Equ. 1}]$$

Some lightly loaded (usually less than 10% of the nominal load) converters were found to operate in discontinuous mode, causing a ripple that was out of specification (figure 14). To reduce this ripple, the converter must operate in continuous mode. This can be achieved either by the addition of preload resistors (at expense of reduced efficiency) or with the reduction of the power range of the lightly loaded converters. The latter solution was successfully exercised with the reduction by a factor 2 of the switching frequency. The correlated noise of the slow integrators system was significantly reduced, as seen on the corresponding correlation charts (figure 15).

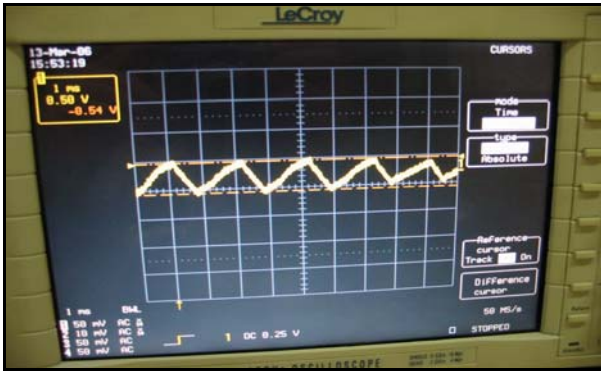


Figure 14: 500mV<sub>pp</sub>, 500 Hz voltage ripple of a weakly loaded converter that operates in discontinuous mode.

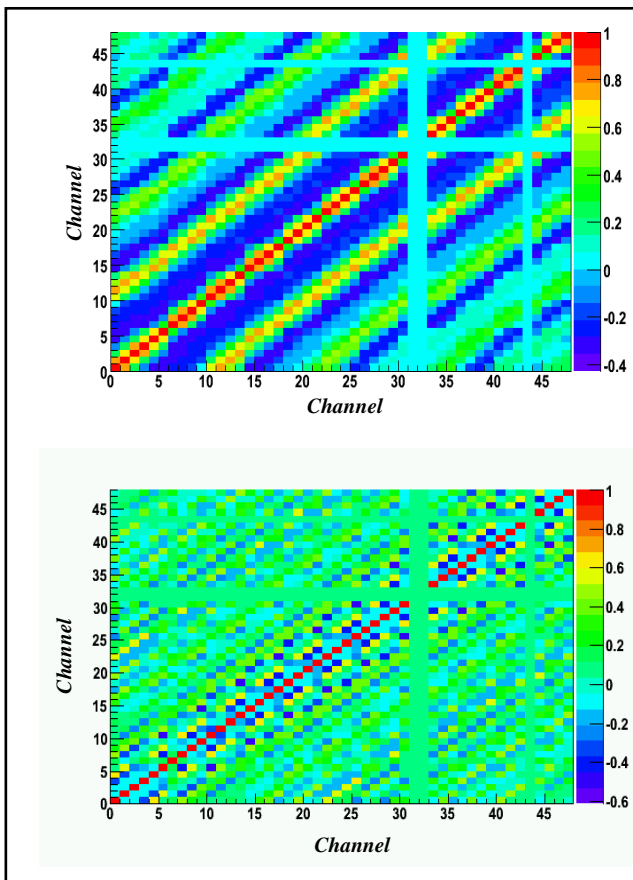


Figure 15: correlation charts of the slow integrators pedestals for a power supply operating in discontinuous mode (top) and in continuous mode (bottom).

### CONCLUSION

The electrical and mechanical constraints set on the Tile Calorimeter low voltage power supplies imposed the need for compact, custom made switched mode converters.

The maximum noise that the Tile Calorimeter can afford is specified for the fast readout system and for the slow calibration and monitoring system. The custom made power supply must be compatible with these system noise specifications.

The front-end electronics of the Tile Calorimeter turned out to be very sensitive to high frequency common mode current on the low voltage lines. Noise currents 20 dB below the limits commonly in use in ATLAS are needed to achieve the required performance. The addition of common mode filters on each converter output is needed to reduce the common mode current to an acceptable level.

One obtains the best fast readout noise performance with the addition of common mode chokes on each converter output. Those are however too bulky for the envelope of the power supply. Instead of this, the addition of two ferrites on each low voltage pair of cable between the power supply and the drawer was exercised. It appeared to be effective to block the high frequency common mode currents and to achieve the required noise performance.

The slow calibration and monitoring system is sensitive to the ripple on the low voltage lines. Correlation charts put in evidence the presence of low frequency ripple in the system. To maintain the ripple within specifications, the power range of the converters that deliver less power is reduced in order to raise their operating point into continuous mode. For this the switching frequency of these converters was reduced to half of its initial value.

The noise properties of the DC/DC converters were compared with the susceptibility of the fast and slow readout electronics. From this a noise coupling model was established, and different filtering solutions were exercised. Among those, the use of ferrites and common mode decoupling capacitors appeared to be most suitable method that allows operating the front-end electronics within the detector noise specifications.

### REFERENCES

- [1] The Tilecal Collaboration, ATLAS - Tile Calorimeter Technical Design Report, CERN/LHCC/96-42 (1996).
- [2] “Design of the front-end analog electronics for the ATLAS tile calorimeter”, K. Anderson et al., Nucl. Instr. and Meth. A, Vol. 551 (2005), pp. 469–476.
- [3] “The Embedded Local Monitor Board (ELMB) in the LHC Front-end I/O Control System”, B. Hallgren, 7<sup>th</sup> Workshop on Electronics for LHC Experiments, LECC2001.
- [4] “Overview of the ATLAS Electromagnetic Compatibility Policy”, G. Blanchot., 10<sup>th</sup> Workshop on Electronics for LHC Experiments, LECC2004.